

# Nonlinearity-induced optical torque

Ivan Toftul,<sup>1,2,\*</sup> Gleb Fedorovich,<sup>2</sup> Denis Kislov,<sup>2,3,4</sup> Kristina Frizyuk,<sup>2</sup> Kirill Koshelev,<sup>1</sup> Yuri Kivshar,<sup>1</sup> and Mihail Petrov<sup>2</sup>

<sup>1</sup>*Nonlinear Physics Center, Research School of Physics, Australia National University, Canberra ACT 2601, Australia*

<sup>2</sup>*School of Physics and Engineering, ITMO University, St. Petersburg 197101, Russia*

<sup>3</sup>*Riga Technical University, Institute of Telecommunications, Riga 1048, Latvia*

<sup>4</sup>*Center for Photonics and 2D Materials, Moscow Institute of Physics and Technology, Dolgoprudny 141700, Russia*

(Dated: October 11, 2022)

Optically-induced mechanical torque leading to the rotation of small objects requires the presence of absorption or breaking cylindrical symmetry of a scatterer. A spherical non-absorbing particle cannot rotate due to the conservation of the angular momentum of light upon scattering. Here, we suggest a novel physical mechanism for the angular momentum transfer to non-absorbing particles via nonlinear light scattering. The breaking of symmetry occurs at the microscopic level manifested in *nonlinear negative optical torque* due to the excitation of resonant states at the harmonic frequency with higher projection of angular momentum. The proposed physical mechanism can be verified with resonant dielectric nanostructures, and we suggest some specific realizations.

*Introduction.* The rotation and spinning of micro- and nanoscale objects is one of the central goals of optical manipulation since the discovery of optical tweezers [1–8], utilized in controlling biological systems [9–11], atoms [12, 13], and nanoscale objects [14–18]. The transfer of angular momentum from light to matter results in a mechanical torque acting on a scatterer [19–22], being proportional to a difference between the angular momenta absorbed and re-scattered by the object. nonzero mechanical torque can appear due to the lack of rotational symmetry [23–26] or the presence of absorption [27, 28]. The direction and sign of the mechanical torque is defined by the imbalance condition, and it can be opposite to the projection of the incident angular moment of light leading to *negative optical torque* (NOT) [29]. The appearance of linear NOT has recently been studied both theoretically [29–31] and experimentally [32–35].

Rapid development of all-dielectric nanophotonics [36–39] brings novel opportunities for optical manipulation. In contrast to nanoplasmonics, dielectric materials have lower Ohmic losses [40], which are required for realizing optical rotation of cylindrically symmetric structures [27, 28]. However, dielectric structures offer unique opportunities for observing nonlinear optical processes such as second harmonic generation (SHG) or third-harmonic generation (THG) due to large values of bulk nonlinear susceptibilities. It is also possible to observe experimentally SHG in trapped particles [41, 42]. Recently, the dramatic enhancement of the SHG efficiency for resonant all-dielectric nanostructures was reported [43–47]. Here, we suggest utilizing the SHG for a transfer of angular momenta of light to scatterers via nonlinear optical process. The generated *second harmonic (SH) field also may carry the angular momenta* and, thus, provides a contribution to the mechanical torque. We predict that the angular momentum imbalance between the fields at the fundamental and SH frequencies can lead to an op-

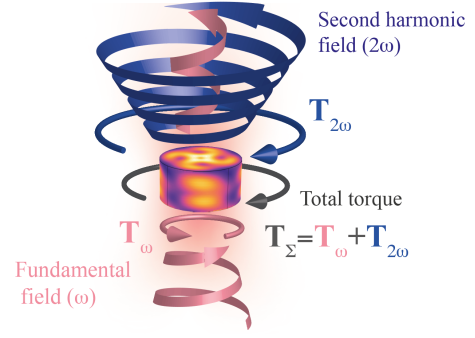


FIG. 1. General concept. Circular polarized light at the frequency  $\omega$  is launched onto a cylindrical dielectric particle and generates second-harmonic fields at the frequency  $2\omega$  that might have different angular momentum due to a crystalline lattice structure, producing a nonlinearity-induced optical torque enhanced by the Mie resonances.

tical torque even for non-absorbing particles with cylindrical symmetry (Fig. 1), and its sign can change from positive to *negative* with respect to the incident field angular momentum.

*Nonlinearity-induced optical torque.* We start with considering circularly polarized plane wave with frequency  $\omega$  scattered on a dielectric particle possessing the azimuthal symmetry (see Fig. 1). The plane wave is incident along the axis of the symmetry and carries the momentum of light of  $m_{\text{inc}}\hbar$  per photon. Due to the symmetry of the problem the optical torque  $\mathbf{T}^{(\omega)}$  acting on the particle at the fundamental frequency is exactly proportional to the absorption cross section [27, 28] and, in terms of canonical spin angular momenta density, one can write  $\mathbf{T}^{(\omega)} = c/n_0 \cdot \sigma_{\text{abs}} \mathbf{S}^{(\omega)}$ , where  $\mathbf{S}^{(\omega)} = m_{\text{inc}}/(2\omega) \cdot \varepsilon \varepsilon_0 [E_0^{(\omega)}]^2 \mathbf{e}_z$  is the canonical spin angular momenta density [48] with azimuthal number  $m_{\text{inc}} = \pm 1$  for right(left) circular polarization and  $n_0 = \sqrt{\varepsilon\mu}$  is the refractive index of the host media;  $\sigma_{\text{abs}}$  is the total absorp-

tion cross section. For a nonlinear process in dielectric particles, the energy loss at the fundamental harmonic (FH) frequency occurs due to the harmonic generation, so  $\sigma_{\text{abs}} \rightarrow \sigma_{\text{SHG}}$ . With the consideration of SHG being a dominant nonlinear process [49], one should also account for the angular momenta carried out by the SH field (Fig. 1). Hence, there are two components of the optical nonlinear torque

$$\mathbf{T} = \mathbf{T}^{(\omega)} + \mathbf{T}^{(2\omega)}, \quad (1)$$

where  $\mathbf{T}^{(\omega)}$  and  $\mathbf{T}^{(2\omega)}$  are the torques generated by the field at FH and SH. The interference terms with nonzero frequencies are averaged to zero [50].

For the particles possessing an azimuthal symmetry with negligible Ohmic losses excited at frequencies away from two and three photon absorption regions [51], torque on the FH is defined by the amount of energy spent on the SHG process. By decomposing SH field into the series of vector spherical harmonics (VSH) it is possible to express SH generation cross section  $\sigma_{\text{SHG}}$  in terms of the radial electromagnetic energy density in magnetic and electric multipoles in the far field  $W_{mj}^{\text{E}}$  and  $W_{mj}^{\text{M}}$  [43, 50], so torque at the FH is

$$T_z^{(\omega)} = m_{\text{inc}} T_0 \frac{\sigma_{\text{SHG}}}{\sigma_{\text{geom}}} = \frac{m_{\text{inc}} T_0}{\sigma_{\text{geom}} [k(2\omega)]^2} \sum_{jm} (W_{mj}^{\text{E}} + W_{mj}^{\text{M}}), \quad (2)$$

where  $k(2\omega) = n_0 2\omega/c$ ,  $\sigma_{\text{geom}}$  is the geometric cross section,  $m_j$  are the projection and the total angular momentum numbers, and  $T_0 = 0.5 \varepsilon \varepsilon_0 [E_0^{(\omega)}]^2 \sigma_{\text{geom}} / k(\omega)$ , is the maximal torque which can be transferred to a plate of area  $\sigma_{\text{geom}}$  once all the momentum of the incident field is absorbed. Coefficients  $W_{mj}^{\text{E}}$  and  $W_{mj}^{\text{M}}$  depend on the overlap integral between the nonlinear polarization  $\mathbf{P}^{(2\omega)} = \varepsilon_0 \hat{\chi}^{(2)} \mathbf{E}^{(\omega)} \mathbf{E}^{(\omega)}$  and field of the SH mode in the volume of the particle [50]. Thus  $W_{mj}^{\text{E}}$  and  $W_{mj}^{\text{M}}$  contains all the information about nonlinear response.

The torque on the SH frequency can be derived by the calculating the change of the total angular momentum flux tensor  $\hat{\mathcal{M}}^{(2\omega)}$  on the SH as  $\mathbf{T}^{(2\omega)} = \oint_{\Sigma} \hat{\mathcal{M}}^{(2\omega)} \cdot \mathbf{nd}S$  [19, 20, 22, 52–54]. Surface integration is performed over arbitrary closed surface  $\Sigma$  which contains the scatterer, and  $\mathbf{n}$  is the outer normal to that surface. This integral can be taken once the fields are decomposed into the VSH series [55–58] and the total torque can be written in a compact and elegant way which underpins the physics behind nonlinearity-induced optical torque [50]:

$$T_z = T_z^{(\omega)} + T_z^{(2\omega)} \quad (3)$$

$$= \frac{1}{2} T_0 \frac{1}{\sigma_{\text{geom}} [k(2\omega)]^2} \sum_{jm} (2m_{\text{inc}} - m) [W_{mj}^{\text{E}} + W_{mj}^{\text{M}}].$$

Eq. (3) is the central result of this work. Generation of SH photon in the particular VSH state results in (i) adding a torque corresponding to the spins of two photons absorbed at the FH and (ii) adding a recoil torque

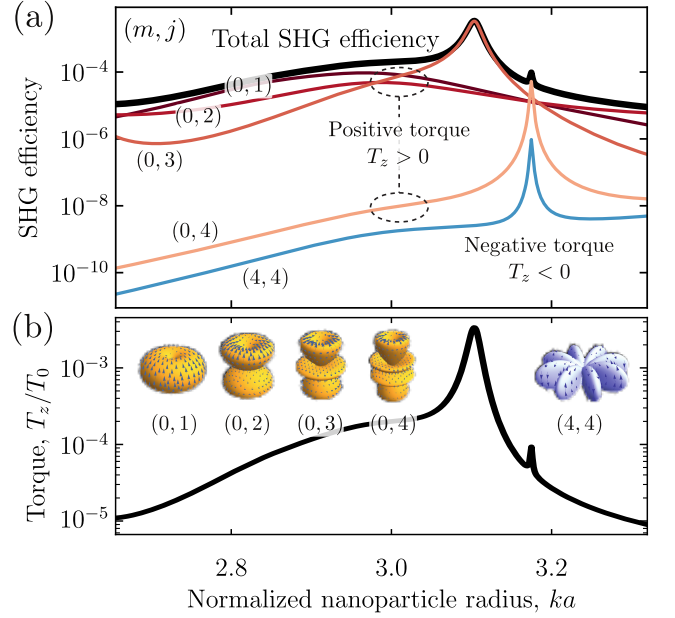


FIG. 2. Exact solution for a dielectric sphere. (a) SHG efficiency ( $\sigma_{\text{SHG}}/\sigma_{\text{geom}}$ ) of a spherical GaAs nanoparticle with refractive indices  $n_p^{(\omega)} = 3.28$ ,  $n_p^{(2\omega)} = 3.56$  as a function of its radius. The colored lines show the contribution of different multipolar channels labeled as  $(m, j)$ . The pump wavelength is 1550 nm. The multipoles with  $m = 0$  and  $m = 4$  provide contribution to positive and negative optical torques, respectively. (b) Total optical torque acting on the nanoparticle due to SHG.

from SH photons emitted with the total angular momentum projection  $m$ . This nonlinear optomechanical effect has not been discussed in the literature and is proposed for the first time, to the best of our knowledge.

*Selection rules.* For the in-depth analysis of Eq. (3) we use the symmetry analysis and multipolar decomposition [43, 59–62]. The imbalance between the angular momentum projections in Eq. (3) immediately shows that there can appear a nonzero torque induced by nonlinear optical generation process results. Its sign with respect to  $m_{\text{inc}}$  strongly depends on the exact multipolar content of SH field. Most of these components are zero due to the strict selection rules on  $m$  during SHG [43, 61, 63–65] imposed by the symmetry of the particle and the crystalline lattice, which can be explicitly seen from the overlapping integral in  $W_{mj}^{\text{E,H}}$  [50]. In order to illustrate the mechanism of NOT appearance, we consider individual crystalline structures made of GaAs which is a common optical material possessing strong second-order nonlinear optical response. Its zinc-blende lattice structure with  $T_d$  symmetry provides a single independent component of the nonlinear tensor  $\chi_{xyz}^{(2)}$  [66–69] once the lattice is oriented such that  $[001] \parallel \hat{\mathbf{e}}_z, [100] \parallel \hat{\mathbf{e}}_x$ .

The symmetry of GaAs lattice along with the axial symmetry of the nanoparticle dictates that only  $m =$

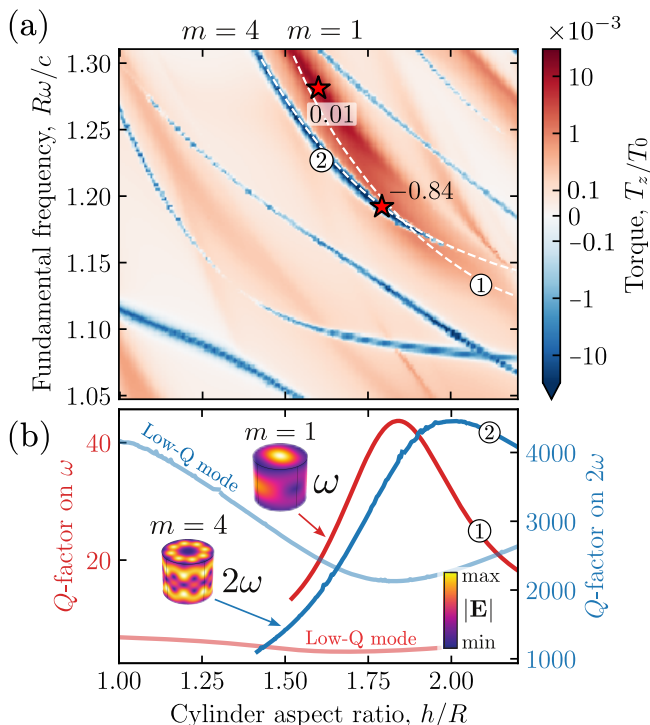


FIG. 3. (a) Total spinning torque on a cylinder with a fixed radius  $R = 250$  nm made of GaAs with refractive index  $n_{\text{cyl}} = 3.5$  placed in air as a function of dimensionless fundamental frequency  $R\omega/c$  and aspect ratio  $h/R$ , where  $h$  is the cylinder height. Two red stars shows maximal positive and maximal negative values of the torque. Notably, the maximal negative torque coincide with the intersection of the two eigenmodes on FH and SH (white dashed lines), which gives double resonant condition for the nonlinearity-induced optical torque. (b) The  $Q$ -factors of these eigenmodes are shown, which have  $m = 4$  on SH and  $m = 1$  on FH. Light blue and light red lines show the  $Q$ -factors of the leaky modes near high- $Q$  modes. Electric field amplitude is  $E_0^{(\omega)} = 8.68 \cdot 10^7$  V/m.

$0, \pm 4$  for incident RCP (LCP) wave are allowed in the SH field, i.e.  $2m_{\text{inc}}$  from the incident field and  $\pm 2$  from the  $\hat{\chi}_{\text{GaAs}}^{(2)}$  tensor (see Supplemental Material for  $\hat{\chi}_{\text{GaAs}}^{(2)}$  explicitly written in cylindrical coordinates [50] and also Refs. [43, 70]). Now from Eq. (3) one can see that for the RCP incident field, which has azimuthal number  $m_{\text{inc}} = 1$ , harmonics with  $m = 0$  provide a positive contribution to the total torque since  $2m_{\text{inc}} - m = 2$  ( $T_z^{(\omega)} > 0$ ,  $T_z^{(2\omega)} = 0$ ), while with  $m = 4$  provide a negative contribution since  $2m_{\text{inc}} - m = -2$  ( $T_z^{(2\omega)} = -2T_z^{(\omega)}$ ) and the recoil torque at SH overcomes the torque at FH.

We next apply these selection rules to SHG in a spherical GaAs particle (including dispersion relations). The particle radius was chosen in the range from 200 nm to 250 nm at the excitation wavelength of 1550 nm. For chosen parameters the excitation is resonant with magnetic dipole mode at the fundamental frequency. The SH field has dominant  $j = 1 \dots 4$  multipolar terms shown in Fig. 2

(b) inset, and their contribution in the overall SHG power are shown in Fig. 2 (a), where SHG efficiency  $\sigma_{\text{SHG}}/\sigma_{\text{geom}}$  is plotted. The magnetic and electric multipole counterparts are not specified in the plot. As discussed above only  $m = 0$  and  $m = 4$  components are present in the SH field. One can see that the major contribution to the SHG signal is governed by the harmonics with  $m = 0$ , while the hexadecapolar harmonic  $j = 4, m = 4$  providing a negative torque contribution is very weak. Thus, the SHG in GaAs spherical particles results in *positive* optical torque (see Fig. 2 (b)) reproducing the SH efficiency spectra according to Eq. (3).

*Negative optical torque enabled by high- $Q$  modes.* The multipole content of SH field can be modified and controlled by designing the resonator shape [71–73]. In the view of this work, we aim at enhancing the contribution of  $m = 4$  modes in the SH field, which can enable appearance of *negative* optical torque. That can be achieved by lifting degeneracy between modes with different  $m$ , utilizing Mie modes with the high total angular momentum  $j$  and quasi-bound states in the continuum (qBIC) with high- $Q$  factors and ability to enhance light-matter interaction in the nanoscale structures [74–77]. The qBIC states can be easily observed in cylindrical particles by variation of height to radius ratio preserving the axial symmetry of the system. The Friedrich-Wintgen mechanism [78] allows interaction of different modes with the same  $m$  via the radiation continuum resulting in the formation of high- $Q$  qBIC modes along with low- $Q$  modes. Fig. 3 (b) shows the  $Q$ -factor of the resonant modes tuned at the FH with  $m = 1$  and at SH with  $m = 4$ , which provides a double resonance condition. The dominating contribution of qBIC modes in the SH spectrum immediately leads to the appearance of negative optical torque (see Fig. 3 (a)) close to  $m = 4$  modes excitation as soon as the recoil contribution of SHG with  $m = 4$  prevails over the torque due to generation of mode with  $m = 0$ . Moreover, the resonant character of the effect provides switching of the optical torque from positive to negative in a very narrow range of parameters.

Excitation of high- $Q$  resonant states leads to the drastic increase of the second harmonic efficiency and optical torque in accordance to Eq. (2). The estimation based on the coupled mode theory [76] gives (see SM [50]):

$$\frac{\sigma_{\text{SHG}}}{\sigma_{\text{geom}}} \simeq 10^{-8} Q_1^2 Q_2 \frac{I_0^{(\omega)}}{1[\text{GW}/\text{cm}^2]}, \quad (4)$$

where  $I_0^{(\omega)} \approx 1.3$  GW/cm<sup>2</sup> is the intensity of the pump field, the  $Q_{1,2}$  are the qBICs  $Q$ -factors on the FH and SH, correspondingly (see Fig. 3). In the steady-state regime, the optical torque leads to the rotation of the object at a constant frequency limited by the viscous friction. For a dielectric cylinder in water estimations give us  $\Omega_{\text{cyl}} \sim 10^5$  rad/s, for the double resonance condition with  $Q_1 \approx 50$  and  $Q_2 \approx 1000$ .

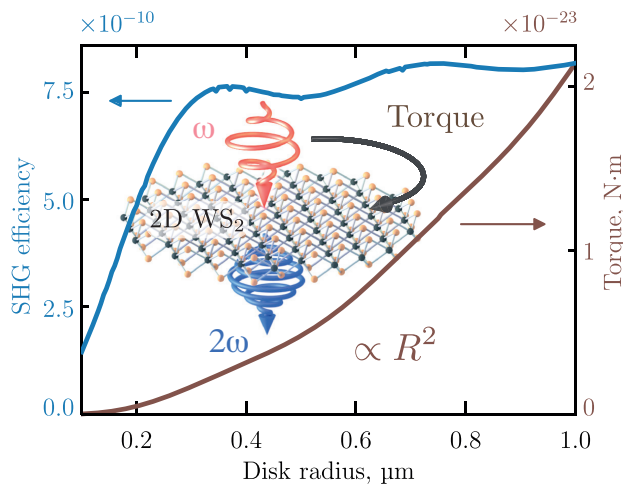


FIG. 4. SHG generation and induced optical torque for  $\text{WS}_2$  flakes. Shown are SHG efficiency  $\sigma_{\text{SHG}}/\sigma_{\text{geom}}$  as a function of the flake size (blue) and induced nonlinear torque (brown). Intensity of the incident field is  $E_0^{(\omega)} = 8.68 \cdot 10^7$  V/m, and wavelength is 1550 nm. Inset: proposed geometry for experimental realization.

*Rotation of TMDC flakes.* The rotation motion of cylindrical structures is unstable for  $h/R \gg 1$ , losing its top-like stability and preventing experimental observation of the proposed effect. The critical AS can be found by setting the equal transverse and longitudinal moments of inertia, which gives  $h/R = \sqrt{3}$ . (see SM [50]). In this view, the rotation of atomically thin non-absorptive disks made of two-dimensional (2D) material is deprived of such limitation. The transition metal dichalcogenides (TMDC) are known as an efficient platform for flat nonlinear optics [79]. The recent experimental successes in TMDC stable floating on top of liquids [80, 81] inspires us for suggesting the potential geometry of the experiment shown in Fig. 4. The circle structure cut of 2D TMDC flake floating over liquid and illuminated by the laser and resulting in SHG. The  $D_{3h}$  symmetry of the crystalline lattice provides the following nonzero components of nonlinear tensor  $\chi_{xxx}^{(2)} = -\chi_{xyy}^{(2)} = -\chi_{yyx}^{(2)} = -\chi_{yxy}^{(2)} = \chi_{2D}^{(2)}$  [67], which provide that SH modes with  $m = \mp 1$  are dominantly generated under right(left)  $m_{\text{inc}} = \pm 1$  circular excitation [67]. Then the difference between the angular momenta of the generated SH field and the incident field is always negative and the torque is directed along the with incident angular momenta (positive optical torque) and equals to  $T_z = \pm 2c/n_0 \cdot \sigma_{\text{SHG}}$ . In Fig. 4 the dependence of the SHG efficiency on the radius of the TMDC structure is shown. The pump wavelength is 1550 nm with the pump power flux of  $2 \text{ GW/cm}^2$  which also lies below the two-photon absorption threshold. The nonlinear tensor coefficient is  $\chi_{2D}^{(2)} = 50 \text{ pm/V}$  [82], while the refractive index at the FH and SH frequency is 2.75 and 3.12 respectively [83] which corresponds to  $\text{WS}_2$  material. From Fig. 4 (b) one

can see that the SHG efficiency tends to a constant value with the increase of the structure size corresponding to the efficiency of an infinite sheet. The torque related to the generation of the SH increases quadratically with the structure size. The estimation of the rotation frequency gives  $\Omega_{2D} \sim 0.1 \text{ rad/s}$  [50].

*Discussions.* The proposed mechanism of nonlinear optical torque occurs to the breaking cylindrical symmetry at the microscopic level, i.e. accounting for the crystal lattice symmetry. Indeed, in the SHG process the rule of the momentum projection conservation is satisfied [84] with correction to additional momentum provided by the susceptibility tensor written in the cylindrical coordinates [50]. The proposed mechanism of nonlinearity-induced torque can be observed via other nonlinear processes such as the THG or higher-harmonic generation. For example, for silicon nanostructures ( $O_h$  lattice symmetry) the SHG process is suppressed while THG is quite strong. The  $\hat{\chi}^{(3)}$  tensor provides the additional momentum  $m = \pm 4$  in the third harmonic field in full analogy to the SHG. We also should stress that the THG in isotropic materials will not induce optical torque as the  $\hat{\chi}^{(3)}$  tensor has specific form [67] which does not give additional angular momenta projection to the field.

Finally, the generation of a nonlinear torque requires quite strong excitation intensities up to  $1 \text{ GW/cm}^2$ . For such intensities, multiphoton absorption can contribute into overall losses leading to a parasitic optical torque not related to the generation of nonlinear fields. Thus, the proposed mechanism in can become possible once two-photon energy is below the band gap  $2\hbar\omega < E_g$ , and two-photon absorption is suppressed which is for room temperature  $E_g^{\text{GaAs}} \simeq 1.4 \text{ eV}$  corresponding to 872 nm.

*Conclusion.* We have presented the general theory of nonlinearity-induced optical torque, originating from the angular momentum transfer from the photonic field to a nanostructure via harmonics generation. We have demonstrated that a nonzero optical torque can appear for the case of a non-absorptive dielectric structures with a rotational symmetry, and the resulting angular frequency can be as high as 100 kHz. Additionally, the stable rotation of circular TMDC flakes of single-layer  $\text{WS}_2$  under the circularly polarized light excitation is also possible. We believe that our work paves a way towards novel intriguing phenomena driven by nonlinearity-induced optomechanical manipulation.

We thank R. Quidant and A. Solntsev for useful comments, and K. Dholakia for references. The work is partially supported by the Program Priority 2030. D.K. acknowledges the Latvian Council of Science (project No. lzp-2021/1-0048). I.T. and Y.K. acknowledge a support from the Australian Research Council (the grant DP210101292), the International Technology Center Indo-Pacific (ITC IPAC) and Army Research Office (contract No. FA520921P0034).

\* [toftul.ivan@gmail.com](mailto:toftul.ivan@gmail.com)

- [1] A. Ashkin, Acceleration and Trapping of Particles by Radiation Pressure, *Phys. Rev. Lett.* **24**, 156 (1970).
- [2] A. Ashkin and J. M. Dziedzic, Optical Levitation by Radiation Pressure, *Appl. Phys. Lett.* **19**, 283 (1971).
- [3] A. Ashkin and J. M. Dziedzic, Stability of optical levitation by radiation pressure, *Appl. Phys. Lett.* **24**, 586 (1974).
- [4] A. Ashkin and J. M. Dziedzic, Optical Levitation of Liquid Drops by Radiation Pressure, *Science* **187**, 1073 (1975).
- [5] A. Ashkin, J. M. Dziedzic, J. E. Bjorkholm, and S. Chu, Observation of a single-beam gradient force optical trap for dielectric particles, *Opt. Lett.* **11**, 288 (1986).
- [6] S. Chu, L. Hollberg, J. E. Bjorkholm, A. Cable, and A. Ashkin, Three-dimensional viscous confinement and cooling of atoms by resonance radiation pressure, *Phys. Rev. Lett.* **55**, 48 (1985).
- [7] J. P. Gordon and A. Ashkin, Motion of atoms in a radiation trap, *Phys. Rev. A* **21**, 1606 (1980).
- [8] A. Ashkin, Trapping of Atoms by Resonance Radiation Pressure, *Phys. Rev. Lett.* **40**, 729 (1978).
- [9] H. Zhang and K.-K. Liu, Optical tweezers for single cells, *J. R. Soc. Interface* **5**, 671 (2008).
- [10] K. Dholakia, B. W. Drinkwater, and M. Ritsch-Marte, Comparing acoustic and optical forces for biomedical research, *Nat. Rev. Phys.* **2**, 480 (2020).
- [11] F. M. Fazal and S. M. Block, Optical tweezers study life under tension, *Nat. Photonics* **5**, 318 (2011).
- [12] A. M. Kaufman and K.-K. Ni, Quantum science with optical tweezer arrays of ultracold atoms and molecules, *Nat. Phys.* **17**, 1324 (2021).
- [13] M. E. Kim, T.-H. Chang, B. M. Fields, C.-A. Chen, and C.-L. Hung, Trapping single atoms on a nanophotonic circuit with configurable tweezer lattices, *Nat. Commun.* **10**, 1 (2019).
- [14] O. M. Maragò, P. H. Jones, P. G. Gucciardi, G. Volpe, and A. C. Ferrari, Optical trapping and manipulation of nanostructures, *Nat. Nanotechnol.* **8**, 807 (2013).
- [15] Y. Shi, Q. Song, I. Toftul, T. Zhu, Y. Yu, W. Zhu, D. P. Tsai, Y. Kivshar, and A. Q. Liu, Optical manipulation with metamaterial structures, *Appl. Phys. Rev.* **9**, 031303 (2022).
- [16] N. Kostina, M. Petrov, A. Ivinskaya, S. Sukhov, A. Bogdanov, I. Toftul, M. Nieto-Vesperinas, P. Ginzburg, and A. Shalin, Optical binding via surface plasmon polariton interference, *Phys. Rev. B* **99**, 125416 (2019).
- [17] G. Tkachenko, G. Tkachenko, I. Toftul, C. Esporlas, A. Maimaiti, A. Maimaiti, A. Maimaiti, F. Le Kien, V. G. Truong, V. G. Truong, S. N. Chormaic, S. N. Chormaic, and S. N. Chormaic, Light-induced rotation of dielectric microparticles around an optical nanofiber, *Optica* **7**, 59 (2020).
- [18] I. D. Toftul, D. F. Kornovan, and M. I. Petrov, Self-Trapped Nanoparticle Binding via Waveguide Mode, *ACS Photonics* **7**, 114 (2020).
- [19] J. D. Jackson, *Classical Electrodynamics*, Vol. 1 (1998).
- [20] L. Novotny and B. Hetch, *Principles of Nano-Optics*, Vol. 1 (2010).
- [21] S. M. B. L. Allen, *Optical Angular Momentum* (Taylor & Francis, Andover, England, UK, 2014).
- [22] Q. Ye and H. Lin, On deriving the Maxwell stress tensor method for calculating the optical force and torque on an object in harmonic electromagnetic fields, *Eur. J. Phys.* **38**, 045202 (2017).
- [23] E. Brasselet and S. Juodkazis, Optical angular manipulation of liquid crystal droplets in laser tweezers, *J. Nonlinear Opt. Phys. Mater.* **18**, 167 (2009).
- [24] M. E. J. Friese, T. A. Nieminen, N. R. Heckenberg, and H. Rubinsztein-Dunlop, Optical alignment and spinning of laser-trapped microscopic particles, *Nature* **394**, 348 (1998).
- [25] S. H. Simpson, D. C. Benito, and S. Hanna, Polarization-induced torque in optical traps, *Phys. Rev. A* **76**, 043408 (2007).
- [26] J. Trojek, L. Chvátal, and P. Zemánek, Optical alignment and confinement of an ellipsoidal nanorod in optical tweezers: a theoretical study, *J. Opt. Soc. Am. A, JOSAA* **29**, 1224 (2012).
- [27] P. L. Marston and J. H. Crichton, Radiation torque on a sphere caused by a circularly-polarized electromagnetic wave, *Phys. Rev. A* **30**, 2508 (1984).
- [28] A. Canaguier-Durand, A. Cuche, C. Genet, and T. W. Ebbesen, Force and torque on an electric dipole by spinning light fields, *Phys. Rev. A* **88**, 033831 (2013).
- [29] J. Chen, J. Ng, K. Ding, K. H. Fung, Z. Lin, and C. T. Chan, Negative Optical Torque - Scientific Reports, *Sci. Rep.* **4**, 1 (2014).
- [30] F. G. Mitri, Negative optical spin torque wrench of a non-diffracting non-paraxial fractional Bessel vortex beam, *J. Quant. Spectrosc. Radiat. Transfer* **182**, 172 (2016).
- [31] M. Nieto-Vesperinas, Optical torque on small bi-isotropic particles, *Opt. Lett.* **40**, 3021 (2015).
- [32] F. Han, J. A. Parker, Y. Yifat, C. Peterson, S. K. Gray, N. F. Scherer, and Z. Yan, Crossover from positive to negative optical torque in mesoscale optical matter, *Nat. Commun.* **9**, 1 (2018).
- [33] N. Sule, Y. Yifat, S. K. Gray, and N. F. Scherer, Rotation and Negative Torque in Electrostatically Bound Nanoparticle Dimers, *Nano Lett.* **17**, 6548 (2017).
- [34] K. Diniz, R. S. Dutra, L. B. Pires, N. B. Viana, H. M. Nussenzveig, and P. A. M. Neto, Negative optical torque on a microsphere in optical tweezers, *Opt. Express* **27**, 5905 (2019).
- [35] D. Hakobyan and E. Brasselet, Left-handed optical radiation torque, *Nat. Photonics* **8**, 610 (2014).
- [36] G. P. Zograf, G. P. Zograf, M. I. Petrov, S. V. Makarov, Y. S. Kivshar, and Y. S. Kivshar, All-dielectric thermophotonics, *Adv. Opt. Photonics* **13**, 643 (2021).
- [37] D. G. Baranov, D. A. Zuev, S. I. Lepeshov, O. V. Kotov, A. E. Krasnok, A. B. Evlyukhin, and B. N. Chichkov, All-dielectric nanophotonics: the quest for better materials and fabrication techniques, *Optica* **4**, 814 (2017).
- [38] Y. Kivshar, All-dielectric meta-optics and non-linear nanophotonics, *Natl. Sci. Rev.* **5**, 144 (2018).
- [39] A. Krasnok, S. Makarov, M. Petrov, R. Savelev, P. Belov, and Y. Kivshar, Towards all-dielectric metamaterials and nanophotonics, in *Proceedings Volume 9502, Metamaterials X*, Vol. 9502 (SPIE, 2015) p. 950203.
- [40] M. Decker and I. Staude, Resonant dielectric nanostructures: a low-loss platform for functional nanophotonics, *J. Opt.* **18**, 103001 (2016).

- [41] L. Malmqvist and H. M. Hertz, Second-harmonic generation in optically trapped nonlinear particles with pulsed lasers, *Appl. Opt.* **34**, 3392 (1995).
- [42] S. Sato and H. Inaba, Second-harmonic and sum-frequency generation from optically trapped KTiOPO<sub>4</sub> microscopic particles by use of Nd:YAG and Ti:Al<sub>2</sub>O<sub>3</sub> lasers, *Opt. Lett.* **19**, 927 (1994).
- [43] K. Frizyuk, I. Volkovskaya, D. Smirnova, A. Poddubny, and M. Petrov, Second-harmonic generation in Mie-resonant dielectric nanoparticles made of noncentrosymmetric materials, *Phys. Rev. B* **99**, 075425 (2019).
- [44] K. Koshelev and Y. Kivshar, Dielectric Resonant Metaphotonics, *ACS Photonics* **8**, 102 (2021).
- [45] L. Carletti, S. S. Kruk, A. A. Bogdanov, C. De Angelis, and Y. Kivshar, High-harmonic generation at the nanoscale boosted by bound states in the continuum, *Phys. Rev. Res.* **1**, 023016 (2019).
- [46] L. Carletti, K. Koshelev, C. De Angelis, and Y. Kivshar, Giant Nonlinear Response at the Nanoscale Driven by Bound States in the Continuum, *Phys. Rev. Lett.* **121**, 033903 (2018).
- [47] L. Bonacina, P.-F. Brevet, M. Finazzi, and M. Celebrano, Harmonic generation at the nanoscale, *J. Appl. Phys.* **127**, 230901 (2020).
- [48] K. Y. Bliokh, A. Y. Bekshaev, and F. Nori, Optical Momentum, Spin, and Angular Momentum in Dispersive Media, *Phys. Rev. Lett.* **119**, 073901 (2017).
- [49] K. M. Ok, E. O. Chi, and P. S. Halasyamani, Bulk characterization methods for non-centrosymmetric materials: second-harmonic generation, piezoelectricity, pyroelectricity, and ferroelectricity, *Chem. Soc. Rev.* **35**, 710 (2006).
- [50] See Supplemental Material at [URL will be inserted by publisher] for the optical torque numerical and analytical calculations details, explicit expressions for the coefficients  $W_{mj}^E$  and  $W_{mj}^H$ ,  $\hat{\chi}^{(2)}$  tensor in cylindrical coordinates, estimations of the SHG efficiency and two- and three-photon absorption cross sections, rigid body rotational dynamics simulations, and detailed section on complex vector spherical harmonics, which includes Refs [19, 20, 43, 54–58, 76, 85–110].
- [51] W. C. Hurlbut, Y.-S. Lee, K. L. Vodopyanov, P. S. Kuo, and M. M. Fejer, Multiphoton absorption and nonlinear refraction of GaAs in the mid-infrared, *Opt. Lett.* **32**, 668 (2007).
- [52] D. J. Griffiths, *Introduction to electrodynamics* (American Association of Physics Teachers, 2005).
- [53] J. Mun, M. Kim, Y. Yang, T. Badloe, J. Ni, Y. Chen, C.-W. Qiu, and J. Rho, Electromagnetic chirality: from fundamentals to nontraditional chiroptical phenomena, *Light Sci. Appl.* **9**, 1 (2020).
- [54] K. Y. Bliokh, A. Y. Bekshaev, and F. Nori, Extraordinary momentum and spin in evanescent waves, *Nature Communications* **5**, 1 (2014), arXiv:1308.0547.
- [55] Z. Li, Z. Wu, T. Qu, H. Li, L. Bai, and L. Gong, Radiation torque exerted on a uniaxial anisotropic sphere: Effects of various parameters, *Opt. Laser Technol.* **64**, 269 (2014).
- [56] Z.-J. Li, Z.-S. Wu, Q.-C. Shang, L. Bai, and C.-H. Cao, Calculation of radiation force and torque exerted on a uniaxial anisotropic sphere by an incident Gaussian beam with arbitrary propagation and polarization directions, *Opt. Express* **20**, 16421 (2012).
- [57] G. Pesce, P. H. Jones, O. M. Maragò, and G. Volpe, Optical tweezers: theory and practice, *Eur. Phys. J. Plus* **135**, 1 (2020).
- [58] F. Borghese, P. Denti, R. Saija, and M. A. Iatì, Radiation torque on nonspherical particles in the transition matrix formalism, *Opt. Express* **14**, 9508 (2006).
- [59] M. Tsimokha, V. Igoshin, A. Nikitina, I. Toftul, K. Frizyuk, and M. Petrov, Acoustic resonators: Symmetry classification and multipolar content of the eigenmodes, *Phys. Rev. B* **105**, 165311 (2022).
- [60] Z. Sadrieva, K. Frizyuk, M. Petrov, Y. Kivshar, and A. Bogdanov, Multipolar origin of bound states in the continuum, *Phys. Rev. B* **100**, 115303 (2019).
- [61] K. Frizyuk, Second-harmonic generation in dielectric nanoparticles with different symmetries, *J. Opt. Soc. Am. B, JOSAB* **36**, F32 (2019).
- [62] K. Frizyuk, E. Melik-Gaykazyan, J.-H. Choi, M. I. Petrov, H.-G. Park, and Y. Kivshar, Nonlinear Circular Dichroism in Mie-Resonant Nanoparticle Dimers, *Nano Lett.* **21**, 4381 (2021).
- [63] M. Finazzi, P. Biagioni, M. Celebrano, and L. Duò, Selection rules for second-harmonic generation in nanoparticles, *Phys. Rev. B* **76**, 125414 (2007).
- [64] S. V. Makarov, M. I. Petrov, U. Zywiets, V. Milichko, D. Zuev, N. Lopanitsyna, A. Kuksin, I. Mukhin, G. Zograf, E. Ubyivovk, D. A. Smirnova, S. Starikov, B. N. Chichkov, and Y. S. Kivshar, Efficient Second-Harmonic Generation in Nanocrystalline Silicon Nanoparticles, *Nano Lett.* **17**, 3047 (2017).
- [65] D. Smirnova, A. I. Smirnov, and Y. S. Kivshar, Multipolar second-harmonic generation by Mie-resonant dielectric nanoparticles, *Phys. Rev. A* **97**, 013807 (2018).
- [66] C. S. Smith, Macroscopic Symmetry and Properties of Crystals, in *Solid State Physics*, Vol. 6 (Academic Press, Cambridge, MA, USA, 1958) pp. 175–249.
- [67] R. Boyd, *Nonlinear Optics* (Elsevier Science, 2020).
- [68] R. C. Miller, Optical second harmonic generation in piezoelectric crystals, *Appl. Phys. Lett.* **5**, 17 (1964).
- [69] P. A. Franken and J. F. Ward, Optical Harmonics and Nonlinear Phenomena, *Rev. Mod. Phys.* **35**, 23 (1963).
- [70] K. Frizyuk, E. Melik-Gaykazyan, J.-H. Choi, M. I. Petrov, H.-G. Park, and Y. Kivshar, Nonlinear Circular Dichroism in Mie-Resonant Nanoparticle Dimers, *Nano Lett.* **21**, 4381 (2021).
- [71] S. Gladyshev, K. Frizyuk, and A. Bogdanov, Symmetry analysis and multipole classification of eigenmodes in electromagnetic resonators for engineering their optical properties, *Physical Review B* **102**, 75103 (2020).
- [72] Z. Sadrieva, K. Frizyuk, M. Petrov, Y. Kivshar, and A. Bogdanov, Multipolar origin of bound states in the continuum, *Physical Review B* **100**, 1 (2019), arXiv:1903.00309.
- [73] T. Liu, R. Xu, P. Yu, Z. Wang, and J. Takahara, Multipole and multimode engineering in Mie resonance-based metastructures, *Nanophotonics* **0**, 1 (2020).
- [74] K. Koshelev, Z. Sadrieva, A. Shcherbakov, Y. Kivshar, and A. Bogdanov, Bound states in the continuum in photonic structures, arXiv [10.3367/UFNe.2021.12.039120](https://arxiv.org/abs/10.3367/UFNe.2021.12.039120) (2022), [2207.01441](https://arxiv.org/abs/2207.01441).
- [75] M. V. Rybin, K. L. Koshelev, Z. F. Sadrieva, K. B. Samusev, A. A. Bogdanov, M. F. Limonov, and Y. S. Kivshar, High-Q Supercavity Modes in Subwavelength Dielectric Resonators, *Phys. Rev. Lett.* **119**, 243901 (2017).

- [76] K. Koshelev, S. Kruk, E. Melik-Gaykazyan, J.-H. Choi, A. Bogdanov, H.-G. Park, and Y. Kivshar, Subwavelength dielectric resonators for nonlinear nanophotonics, *Science* **367**, 288 (2020).
- [77] A. A. Bogdanov, K. L. Koshelev, P. V. Kapitanova, M. V. Rybin, S. A. Gladyshev, Z. F. Sadrieva, K. B. Samusev, Y. S. Kivshar, and M. F. Limonov, Bound states in the continuum and Fano resonances in the strong mode coupling regime, *Advanced Photonics*, *1(1)*, *Adv. Photonics* **1**, 016001 (2019).
- [78] Friedrich H. and Wintgen D., Interfering resonances and BIC, *Physical Review A* **32**, 3231 (1985).
- [79] S. J. McDonnell and R. M. Wallace, Atomically-thin layered films for device applications based upon 2D TMDC materials, *Thin Solid Films* **616**, 482 (2016).
- [80] X.-k. Zhao, R.-w. Chen, K. Xu, S.-y. Zhang, H. Shi, Z.-y. Shao, and N. Wan, Nanoscale water film at a super-wetting interface supports 2D material transfer, *2D Mater.* **8**, 015021 (2020).
- [81] G. Jin, C.-S. Lee, X. Liao, J. Kim, Z. Wang, O. F. N. Okello, B. Park, J. Park, C. Han, H. Heo, J. Kim, S. H. Oh, S.-Y. Choi, H. Park, and M.-H. Jo, Atomically thin three-dimensional membranes of van der Waals semiconductors by wafer-scale growth, *Sci. Adv.* **5**, eaaw3180 (2019).
- [82] J. W. You, S. R. Bongu, Q. Bao, and N. C. Panoiu, Nonlinear optical properties and applications of 2D materials: theoretical and experimental aspects, *Nanophotonics* **8**, 63 (2019).
- [83] G. A. Ermolaev, D. I. Yakubovsky, Y. V. Stebunov, A. V. Arsenin, and V. S. Volkov, Spectral ellipsometry of monolayer transition metal dichalcogenides: Analysis of excitonic peaks in dispersion, *Journal of Vacuum Science & Technology B, Nanotechnology and Microelectronics: Materials, Processing, Measurement, and Phenomena* **38**, 014002 (2019).
- [84] A. Nikitina, A. Nikolaeva, and K. Frizyuk, When does nonlinear circular dichroism appear in achiral dielectric nanoparticles?, arXiv [10.48550/arXiv.2208.00891](https://arxiv.org/abs/10.48550/arXiv.2208.00891) (2022), [2208.00891](https://arxiv.org/abs/2208.00891).
- [85] C. F. Bohren and D. R. Huffman, *Absorption and scattering of light by small particles* (John Wiley & Sons, 2008).
- [86] M. B. Doost, W. Langbein, and E. A. Muljarov, Resonant-state expansion applied to three-dimensional open optical systems, *Phys. Rev. A* **90**, 013834 (2014).
- [87] H. S. Sehmi, W. Langbein, and E. A. Muljarov, Applying the resonant-state expansion to realistic materials with frequency dispersion, *Phys. Rev. B* **101**, 045304 (2020).
- [88] S. V. Lobanov, W. Langbein, and E. A. Muljarov, Resonant-state expansion applied to three-dimensional open optical systems: Complete set of static modes, *Phys. Rev. A* **100**, 063811 (2019).
- [89] D. A. Varshalovich, A. N. Moskalev, and V. K. Khersonskii, *Quantum Theory of Angular Momentum* (World Scientific Publishing Company, Singapore, 1988).
- [90] E. W. Weisstein, Condon-Shortley Phase, *Wolfram Research, Inc.* (2003).
- [91] J. A. Stratton, *Electromagnetic Theory* (John Wiley & Sons).
- [92] COMSOL Documentation (2021), [Online; accessed 2. Jun. 2021].
- [93] C. M. De Witt and J. H. D. Jensen, Über den Drehimpuls der Multipolstrahlung, *Zeitschrift für Naturforschung A* **8**, 267 (1953).
- [94] Z. Li, Z. Wu, T. Qu, H. Li, L. Bai, and L. Gong, Radiation torque exerted on a uniaxial anisotropic sphere: Effects of various parameters, *Optics & Laser Technology* **64**, 269 (2014).
- [95] Z.-J. Li, Z.-S. Wu, and Q.-C. Shang, Calculation of radiation forces exerted on a uniaxial anisotropic sphere by an off-axis incident Gaussian beam, *Optics Express* **19**, 16044 (2011).
- [96] Z.-J. Li, Z.-S. Wu, Q.-C. Shang, L. Bai, and C.-H. Cao, Calculation of radiation force and torque exerted on a uniaxial anisotropic sphere by an incident Gaussian beam with arbitrary propagation and polarization directions, *Optics Express* **20**, 16421 (2012).
- [97] J. P. Barton, D. R. Alexander, and S. A. Schaub, Theoretical determination of net radiation force and torque for a spherical particle illuminated by a focused laser beam, *Journal of Applied Physics* **66**, 4594 (1989), [arXiv:cs/9605103](https://arxiv.org/abs/cs/9605103).
- [98] J. P. Barton, D. R. Alexander, and S. A. Schaub, Internal and near-surface electromagnetic fields for a spherical particle irradiated by a focused laser beam, *Journal of Applied Physics* **64**, 1632 (1988).
- [99] L. D. Landau, J. Bell, M. Kearsley, L. Pitaevskii, E. Lifshitz, and J. Sykes, *Electrodynamics of continuous media*, Vol. 8 (elsevier, 2013).
- [100] toftul, *tensors-in-curvilinear-coordinates* (2022), [Online; accessed 18. Jul. 2022].
- [101] S. Bergfeld and W. Daum, Second-Harmonic Generation in GaAs: Experiment versus Theoretical Predictions of  $\chi_{xyz}^{(2)}$ , *Phys. Rev. Lett.* **90**, 036801 (2003).
- [102] K. Koshelev, *Advanced trapping of light in resonant dielectric metastructures for nonlinear optics*, Ph.D. thesis, Australian National University (2022).
- [103] G. Kristensson, Spherical vector waves (2014).
- [104] T. Weiss and E. A. Muljarov, How to calculate the pole expansion of the optical scattering matrix from the resonant states, *Phys. Rev. B* **98**, 085433 (2018).
- [105] E. A. Muljarov and T. Weiss, Resonant-state expansion for open optical systems: generalization to magnetic, chiral, and bi-anisotropic materials, *Opt. Lett.* **43**, 1978 (2018).
- [106] F. Perrin, Mouvement brownien d'un ellipsoïde - I. Dispersion diélectrique pour des molécules ellipsoïdales, *J. Phys. Radium* **5**, 497 (1934).
- [107] C. R. Cantor and P. R. Schimmel, *Biophysical chemistry: Part II: Techniques for the study of biological structure and function* (Macmillan, 1980).
- [108] S. H. Koenig, Brownian motion of an ellipsoid. a correction to perrin's results, *Biopolymers: Original Research on Biomolecules* **14**, 2421 (1975).
- [109] L. D. Landau and E. M. Lifshitz, *Fluid Mechanics: Landau and Lifshitz: Course of Theoretical Physics, Volume 6*, Vol. 6 (Elsevier, 2013).
- [110] E. A. Coutias and L. Romero, The Quaternions with an application to Rigid Body Dynamics, *UNM Digital Repository* (2004).